Arab J Geosci (2011) 4:259–267
DOI 10.1007/s12517-010-0166-6

ORIGINAL PAPER

Effects of diurnal temperature rhythm on the geothermal regime under the embankment in Qinghai–Tibet plateau

Yinghong Qin · Pei Tang

Received: 25 January 2010 / Accepted: 19 March 2010 / Published online: 23 July 2010

Abstract The objective of this study was to investigate the effects of diurnal temperature fluctuation amplitude (DTFA) on the geothermal regime of the embankment on the Qinghai–Tibet plateau. The investigation was simulated by respectively denoting the diurnal temperatures at the embankment surface, embankment slope, and natural ground surface with sinusoidal waves. The amplitudes of the waves were denoted by 0°C, 5°C, 8°C, and 12°C, respectively. The numerical result shows that the DTFA cannot vary the frequency of the seasonal temperature fluctuation of the underlying soil, but can significantly change the magnitude of the soil's temperature. The changes include: (1) The high DTFA, such as 12°C, can significantly lead to the warming of the soil under the embankment. (2) Interestingly, when the DTFA at ground surface is 5°C, the underlying soil is in a cooler stage compared to when such DTFA is 0°C, 8°C, or12°C. This interesting result means that the documented model which ignores the diurnal temperature rhythm overestimates the warming of the underlying soil at the low DTFA region and underestimates such warming at the high DTFA region. This result also suggests that the soil under the embankment can be cooled down if the DTFA on the ground surface was maintained at or approximately at 5°C.

Keywords Geo-temperature · Diurnal temperature fluctuation amplitude (DTFA) · Cold energy · Warm energy · Thermal regime

Y. Qin (✉) · P. Tang
Department of Civil and Environmental Engineering,
Michigan Technological University,
1400-1295 Townsend Drive,
Houghton, MI 49931, USA
e-mail: yinghong231@gmail.com

Introduction

The geo-temperature under the embankment along the Qinghai–Tibet Line, including the Qinghai–Tibet Railway and Qinghai–Tibet Highway, is a crucial factor determining the performance of the roadway (Cheng et al. 2008b; Ma et al. 2008; Qin et al. 2010; Qin and Zheng 2010; Zhang et al. 2008). Numerical models used to simulate this geo-temperature have been well documented (Li et al. 2009; Zhang et al. 2005a). In these models, the temperatures denoted on the boundary of the embankment slope surface, embankment surface, and natural ground surface were considered as a linear function (the effect of climate warming) plus a sinusoidal wave (the seasonal rhythm). The diurnal temperature fluctuation was not counted.

However, without considering the diurnal temperature rhythm may lead to the underlying soil's temperature being incorrectly predicted because the ground surface temperature in the Qinghai–Tibet Plateau fluctuates seasonally and diurnally. This incorrect prediction of the upper boundary conditions will definitely not guarantee the estimation for the long-term thermal stability of the underlying permafrost. In fact, when the diurnal temperature rhythm is considered, the temperature near the ground surface is completely different. The diurnal temperature rhythm forms a high nonlinear temperature gradient near the ground surface (Armagahni et al. 1987), potentially varying the geothermal regime under the roadway embankment both in the short and long terms. Considering such potential variation, a numerical model based on approximately 9000 hours in situ temperature has been done to estimate the geo-temperature under an embankment along the Qinghai–Tibet Railway (Li et al. 2007; Quan et al. 2006). The result shows that the diurnal temperature fluctuation amplitude (DTFA) does affect the underlying thermal regime in the short term. However, since

9000 hours in situ temperature is of short-term data, this model was unable to capture the long-term effect of DTFA on the geothermal regime. Therefore, it is of necessity to investigate the effect of DTFA on the geothermal regime in the cold region and estimate the geo-temperature under the ground surface which experiences different DTFAs.

This study firstly used a numerical model which assumes the roadway embankment services at regions within different DTFAs to illustrate the geo-temperatures of the soil under the embankment. In the upper boundary, the DTFA at the embankment surface, embankment slope, and natural ground surface are approximated as sinusoidal wave according to the published literature (Andersland and Ladanyi 1994). The DTFAs were denoted by 0°C, 5°C, 8°C, and 12°C, respectively. The numerical result shows that the DTFA cannot vary the seasonal temperature fluctuation characteristics of the underlying soil, but can significantly change the magnitude of the geo-temperature.

This study secondly examined the mechanism of the effect of DTFA on the geothermal regime. The thermal conductivity of unfrozen soil is greater than that of frozen soil because ice conductivity is approximately four times the water conductivity. Therefore, when the DTFA is of lower magnitude, during a given year, the absorbed cold energy is greater than the absorbed warm energy. This net heat loss leads to the underlying soil maintained at a cool state. However, when in warm season, the DTFA is high enough to partially thaw the underlying permafrost layer; during a given year, the absorbed warm energy is greater than the absorbed cold energy because the warmed energy is stored in the permafrost layer. Therefore, the soil under high DTFA is usually in a warmer state compared to that under low DTFA.

Numerical model

The dimension of the computational domain

To investigate the effect of diurnal temperature on the geothermal regime was the purpose of this study. The effects of the embankment height and the embankment strike on geo-temperature under the embankment can be neglected. With this purpose in mind, the geometry of the embankment is not the crucial factor to be considered. Therefore, a numerical simulation for the thermal conditions of the embankment section located at the Beiluhe site can satisfy the investigation purpose. The geological details for this site can be referred to previous works (Ma et al. 2008; Yu et al. 2008).

To simplify the simulation, it is regarded that the embankment is a symmetric geometry (Fig. 1) by neglecting the so-called slope orientation effects, which has been well documented (Chenji et al. 2006; Ya-ling et al. 2008). This neglect is reasonable because the slope orientation effects are

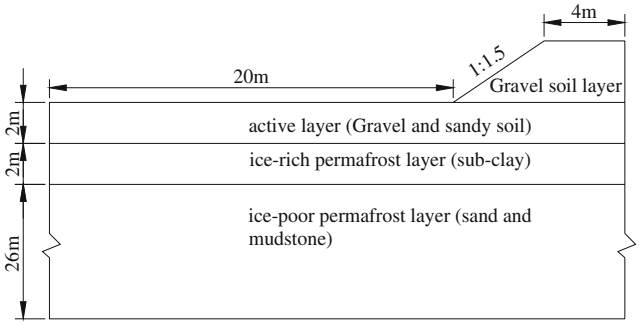

Fig. 1 Computational domain

mainly on both the annual mean temperature and seasonal temperature variation of the embankment slope surface. A simulation for the heat conduct process within both the embankment and underlying soil is degraded to a two-dimensional heat transfer model. In the model, the width and height of the embankment are 3 and 8 m, respectively, and the side slope of the embankment is 1:1.5. The selected physical domain for computation was extended 20 m outward from the embankment toe and −30 m deep downward from the natural ground surface. The depth of the natural permafrost table is −2 m. Underneath the embankment underlies a 2-m thickness of the active layer, and beneath the active layer contains 2-m-thick ice-rich permafrost layer and then 26-m-thick ice-poor permafrost layer.

Material properties

The railway embankment at the Beiluhe site is usually filled by gravel and soil (Zheng et al. 2010). The soil beneath the embankment can be roughly divided into three layers: active layer, consisting of fine sand and silty soil; ice-rich permafrost layers, comprising ground ice and sub-clay; and ice-poor permafrost layer, consisting of weathered mudstone (Zheng et al. 2010). The soil's thermal parameters of these three layers, as well as those of the embankment fill, are shown in Tables 1 and 2 (Zhang 2007).

Table 1 Thermal conductivity parameters of the medium

Stratum	Dry bulk density (kg/m^3)	Total water content (%)	Thermal conductivity (J, mhK)	
			Frozen soil	Thawing soil
Fill (gravel soil layer)	2,060	6	5,040	4,140
Active layer (gravel and sandy soil)	1,880	15	8,692	6,613
Ice-rich permafrost (sub-clay)	1,280	35	7,632	5,112
Ice-poor permafrost (sand and mudstone)	1,800	15	6,552	5,760

Table 2 Heat capacity of the medium

Stratum	Specific heat (J, kgK)								
	20.0–0.0°C	0.0°C to −0.2°C	−0.2°C to −0.5°C	−0.5°C to −1.0°C	−1.0°C to 2.0°C	−2.0°C to −3.0°C	−3.0°C to −5.0°C	−5.0 to −10.0°C	−10.0°C to −20.0°C
Fill	861.7	62,405	9,060	3,497	2,156	1,004	973.5	820.2	706.6
Active layer	1,100	91,594	18,245	8,631.8	3,737.5	1,799	1,367.3	1,032.4	851.8
Ice-rich permafrost	1,608	130,278	35,903	11,864	6,678	6,640	2,702	1,737	1,222
Ice-poor permafrost	1,272	1,267	39,562	16,080	6,160	3,658	2,364	1,476	981.8

Boundary conditions

Temperature boundary conditions of the computational domain are shown in Fig. 2. The temperature of the upper boundary conditions fluctuates seasonally and diurnally and is also affected by global warming. These boundary conditions can be characterized by:

$$T_i = T_0 + 0.02t + A_i \sin\left(\frac{2\pi t}{8760} + \frac{\pi}{2}\right) + D_i \sin\left(\frac{2\pi t}{24} + \frac{\pi}{2}\right) \quad (1)$$

where T_i (°C) (i = 1,2) is the temperature boundaries for the embankment surface (T_2), slope surface T_2, and the natural ground surface (T_1); T_0 (°C) is the mean annual temperature at the Beiluhe permafrost station; t (h) is the simulated time; and A_i and D_i are the seasonal and diurnal temperature fluctuation amplitude, respectively. The first $\pi/2$ means the simulation begins from the warmest day of the first year; the second $\pi/2$ in the first and second sinusoidal expressions signifies that the simulation begins from the warmest time of the warmest day. It merits noting that in Eq. 1, the temperature peak of a given day is at 12:00 P.M. because the last term of this equation is a sinusoidal function with $\pi/2$ phase. If such peak at field appears at 1:00 P.M., 3:00 P.M., or anytime between them, the phase of this term could change from $\pi/2$ to a value such that the diurnal peak in Eq. 1 can exactly match the site-specific condition.

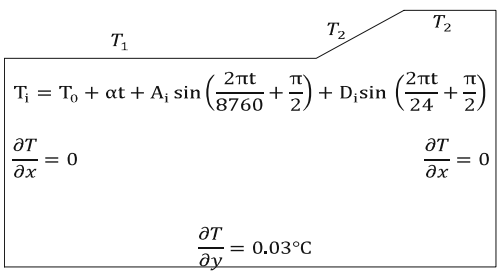

Fig. 2 Boundary conditions of the computational domain

All the parameters in Eq. 1 can be referred to Table 3. According to a documented literature (Qin, 2002), the rate of global warming in the Qinghai–Tibet plateau is given as 0.02°C/year. The mean annual temperature, T_0, is −1.5°C for the natural ground surface and −0.46°C for the surfaces of the slope and embankment. The amplitude of seasonal temperature fluctuation, A_i, is 11.5°C for the natural ground and 14.5°C for the surfaces of the slope and embankment. The diurnal temperature fluctuation amplitude D_i is denoted 0°C, 5°C, 8°C, and 12°C, respectively. For the bilateral boundary conditions, shown in Fig. 2, these boundaries are adiabatic. For the boundary condition at the bottom of the model, a temperature gradient of 0.03°C/m is usually assumed when the geo-temperature in the Beiluhe region was simulated (Ya-ling et al. 2009; Zhang et al. 2005b).

Initial condition

Proper initial temperatures have to be denoted for the soil beneath the ground surface and for the embankment. The initial temperature condition for the soil beneath ground surface is obtained from a long-term (100 years) transient heat transfer solution for the geo-temperatures of the natural ground. This solution was achieved by neglecting the effect of both global warming and diurnal temperature fluctuation in Eq. 1 and by deleting the geometry of the embankment at the computational domain shown in Fig. 1. A detailed calculation for this initial temperature can be referred to the work of Zhang et al. (2005b). The initial temperature for

Table 3 Parameters for Eq. 1

i	Natural ground (°C)		Slope and embank. sur (°C)		D_i (°C)
	T_0	A_i	T_0	A_i	
1	−1.5	11.5	−0.46	14.5	0
2	−1.5	11.5	−0.46	14.5	5
3	−1.5	11.5	−0.46	14.5	8
4	−1.5	11.5	−0.46	14.5	12

the embankment fill is denoted as 2°C since the construction of the embankment completed in September, a month with a mean monthly temperature of 2°C (Li et al. 2006).

Simulation information

The simulation was run using MSC. Marc2005. A 12-node quadratic isoparametric element was used to accelerate the convergent rate. The simulated time t is 10 years. The increment of the time step is 3 h.

Result

Temperature series

The temperature characteristic of the soil under the centerline of the embankment is an important factor determining the stability of the embankment. Under this centerline, the geo-temperatures of the active layer, of the soil around the permafrost table, and of the ice-rich permafrost layer are usually used to estimate the thermal stability of the embankment. In the following, the geo-temperatures at depths of 0.5, 2, and 4 m was recorded and discussed (note that the depth is counted from the natural ground surface rather than the embankment surface).

Under different DTFAs (0°C, 5°C, 8°C, and 12°C), the temperature series of the soils at the same depth exhibit different characteristics. Figures 3a, 4a, and 5a plot the geo-temperatures at depths of 0.5, 2, and 4 m, respectively. These figures show that under different DTFA, the frequency of seasonal temperature fluctuation of the underlying soil is similar but the geo-temperatures at the same depth exhibit different trend. These differences are apparent in that:

1. The geo-temperature of the soil under the 12°C DTFA is greatly larger than that under the 0°C, 5°C, and 8°C DTFAs.
2. The geo-temperature of the soil under the 8°C DTFA is of the lowest temperature approximately in the first 4 years, but after that, this geo-temperature rises.
3. The geo-temperature of the soil under the 5°C DTFA, although slightly higher than that of the soil under the 8°C DTFA at the first 4 years, is of the lowest temperature approximately after the fourth year.

These differences can be more clearly seen from Figs. 3b, 4b, and 5b. The geo-temperatures of the soil under the 5°C, 8°C, and 12°C DTFAs are subtracted by those of the soil under the 0°C DTFA. The subtraction results versus the predicted years are plotted in Figs. 3b, 4b, and 5b, which show that when the DTFA is 5°C, the underlying soil continually cooled down. In contrast, the soil under the 12°C DTFA is progressively warmed up during the predicted years.

Three conclusions can be drawn from a comprehensive look at Figs. 3, 4, and 5. First, when the DTFA is considered, the numerical result for the underlying thermal regime is completely different from the result obtained when ignoring the DTFA. Second, the ground surface experiencing high DTFA, such as 12°C, leads to a warming of the underlying soil. The ground surface experiencing lower DTFA, e.g., 5°C or 8°C, results in a cooling of the underlying soil. Third, in the short term, a ground surface experiencing 8°C DTFA is helpful for the stability of the underlying permafrost, but in the long term, the permafrost under the embankment built in the region with 5°C DTFA will obtain an excellent thermal stability.

Temperature profile of the soil under the centerline of the embankment

When considering the effect of DTFA, the temperature profile of the soil under the centerline of the embankment is completely different. Figure 6 shows the temperature profile in both the warmest and coldest days of the predicted tenth year. The figure shows that:

1. The geo-temperatures under the surface experiencing 12°C DTFA are greatly warming.
2. The geo-temperatures under the ground surface undergoing 5°C DTFA are of the lowest magnitude.

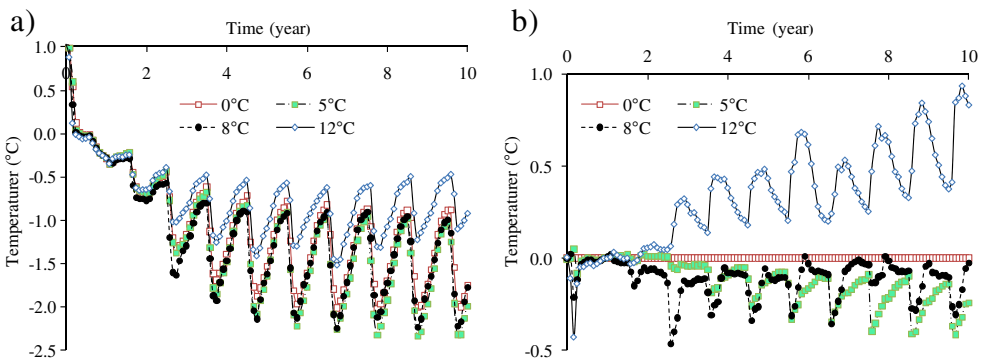

Fig. 3 Geo-temperature series at the depth of −0.5 m beneath the embankment: **a** Temperature series. **b** Predicted time versus the results of using the geo-temperatures under the 0°C DTFA to subtract those under the 5°C, 8°C, and 12°C DTFAs

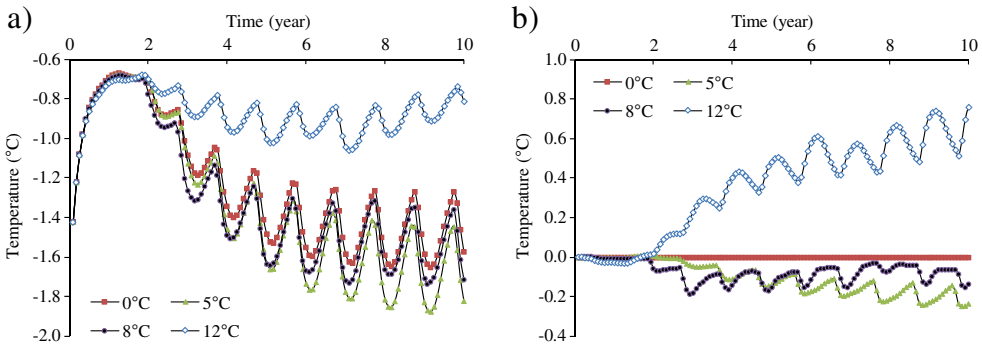

Fig. 4 Geo-temperature series at the depth of −2 m beneath the embankment: **a** Temperature series. **b** Predicted time versus the results of using the geo-temperatures under the 0°C DTFA to subtract those under the 5°C, 8°C, and 12°C DTFAs

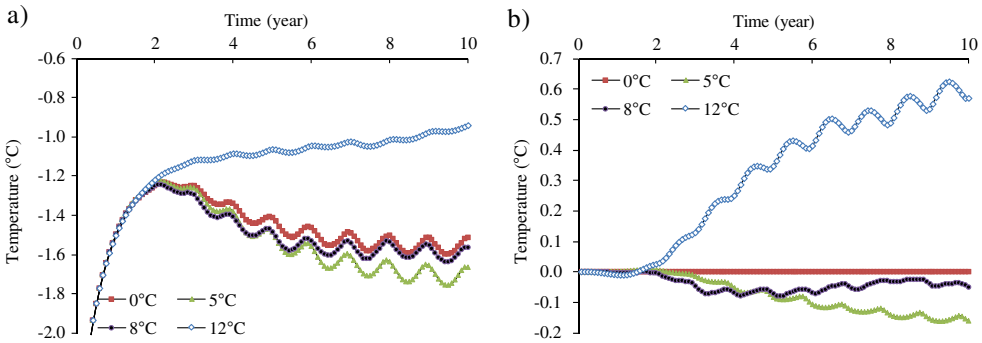

Fig. 5 Geo-temperature series at the depth of −4 m beneath the embankment: **a** Temperature series. **b** Predicted time versus the results of using the geo-temperature under the 0°C DTFA to subtract those under the 5°C, 8°C, and 12°C DTFAs

3. From the 0- to −4-m depth, in cold season, the geo-temperatures under the surface experiencing 0°C and 8°C DTFAs are almost in the same magnitude, but in warm season, the soil under 0°C DTFA is warmer than that under 8°C DTFA.
4. A 12°C DTFA can lead to the underlying soil being warmed downward to approximately −18-m depth, while 0°C, 5°C, and 8°C DTFAs can only affect the geo-temperatures downward to a depth of approximately −13 m.

These four characteristics support the conclusion in "Temperature series". Two additional conclusions can be drawn here. First, if the effect of DTFA on geothermal regime is ignored and the DTFA is of a comparatively lower value such as 5°C or 8°C, the warming of the underlying soil is overestimated, especially in warm season. The warming of the underlying soil is underestimated if the DTFA is of high magnitude, such as 12°C. Second, the higher the DTFA, the deeper is the geothermal regime affected.

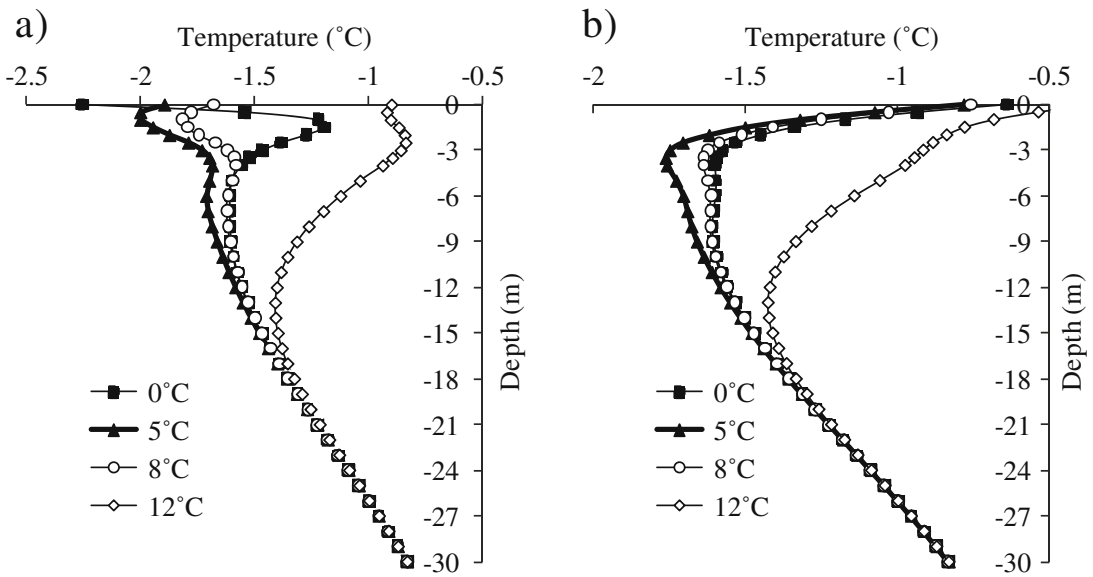

Fig. 6 Geo-temperature profiles at the central borehole. **a** The warmest day of the tenth predicted year. **b** The coldest day of the tenth predicted year

Daily temperature near the original permafrost table

Although the soil under −2-m depth (beneath the centerline of the embankment) does not experience daily temperature rhythm, the temperature at this depth is greatly different in magnitude. Figure 7 shows that the temperature at the depth of 2 m under the ground surface experiences 0°C, 5°C, 8°C, and 12°C on the warmest and coldest days of the tenth predicted year. First, this soil (−2-m depth) does not undergo a daily fluctuation rhythm, even though the ground surface is denoted with DTFA. Second, under individual DTFA, the geo-temperatures at −2-m depth are greatly different in magnitude. The soil under the surface experiencing 12°C DTFA is of the warmest stage compared to that under the ground surface undergoing 0°C, 5°C, and 8°C DTFAs.

The mechanism of the effect of the DTFA on geothermal regime

Lower DTFA

The temperature series, temperature profile, and daily temperature for the soil under the embankment located at regions with different DTFAs have been illustrated above. It is found that the documented model which ignores the diurnal temperature rhythm overestimates the warming of the underlying soil at the low DTFA region and underestimates such warming at the high DTFA region. The mechanism of the effect of the DTFA on the geothermal regime is illustrated in the following.

To understand the mechanism regarding why the underlying soil under the low DTFA is in a cooler state than that under the high DTFA, we make the following assumptions:

1. This low DTFA is low enough so that the diary fluctuation cannot directly lead to the phase change of the underlying permafrost; that is, the warm energy from low DTFA heat transfer is not stored in the permafrost layer.
2. The thermal gradient, grad$T$, near the ground surface can be roughly calculated by dividing the difference between the temperatures at ground surface, T (°C), and at the depth of d (m), T_d (°C), by d. That is, $\text{grad}T|_T = \frac{T-T_d}{d}$. This calculation is schematically shown in Fig. 8.
3. When the temperature at the ground surface changes to $T+f$, the depth of d changes to $d+\varepsilon$. Here, $\varepsilon>0, f>0$. That is, $\text{grad}T|_{T+f} = \frac{T+f-T_{d+\varepsilon}}{d+\varepsilon}$. Setting d as the depth of frost penetration, it is easy to find $d \gg \varepsilon$ according to the Berggren equation (Andersland and Ladanyi 1994). It is known that the soil temperature changes slightly underground compared to the temperature at the ground surface; therefore, $\text{grad}T|_{d-\varepsilon} = \frac{T+f-T_d}{d+\varepsilon}$..

Heat flow difference between ignored and considered DTFA in warm season

Because the period of seasonal temperature rhythm (8760 hours) is two orders greater than that of diurnal temperature (24 h), the temperature of a given day is regarded as a constant if the DTFA is ignored. So when the DTFA is ignored, the daily thermal gradient, $\text{grad}T|_{T_{av}}$, is

$$\text{grad}T|_{T_{av}} = \frac{T_{av} - T_d}{d} \tag{2}$$

where T_{av} is the average daily temperature. When the DTFA is considered, the ground temperature is always deviated from the average daily temperature, T_{av}.

In warm season, set this deviation as $f\,(0 \le f \le D_i)$. It is noted that f varies with time. Because of the anti-symmetry of the sinusoidal wave on a given day, the temperature of the ground surface is $T_{av} - f$ at one specific time and $T_{av} + f$ at another specific time. For example, provided $T_{av} = 10$°C and at $T_{6:00\text{a.m.}} = (10-3)$°C, using Eq. 1 yields $T_{6:00p.m.} =$

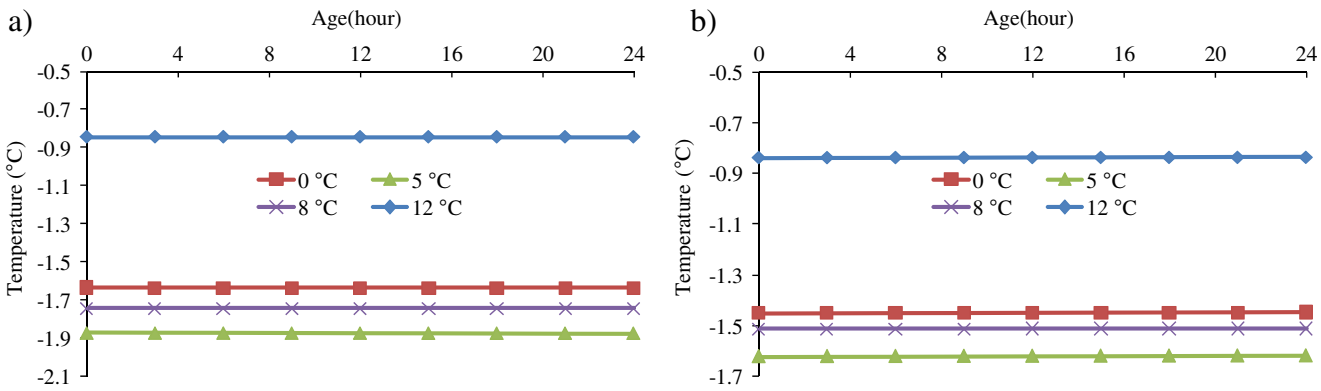

Fig. 7 Daily temperature at −2-m depth. **a** The warmest day of the tenth predicted year. **b** The coldest day of the tenth predicted year

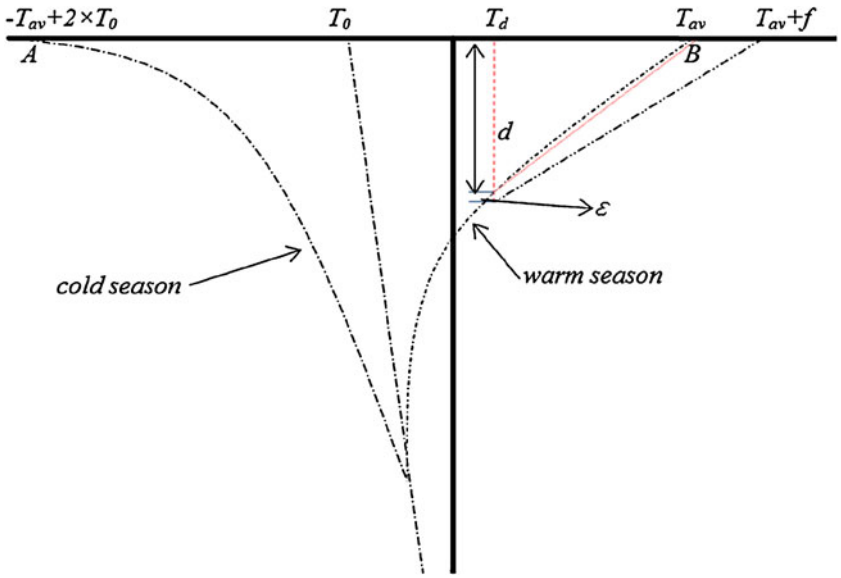

Fig. 8 Geo-temperature profile used to calculate the thermal gradient near ground surface

$(10+3)$°C. According to assumptions 2 and 3, the summation of the thermal gradient at these two specific times is:

$$\text{grad}T|_{T_{av}+f}+\text{grad}T|_{T_{av}-f}=\frac{T_{av}+f-T_{\text{d}}}{d+\varepsilon}+\frac{T_{av}-f-T_d}{d-\varepsilon}. \tag{3}$$

Therefore, for the time at "$T=T_{\text{av}}$" in warm season, the heat flow difference, Δq_{warm}, between the ignored and considered DTFA is

$$\Delta q_{\text{warm}}=-k_{warm}\times[0.5\times(\text{grad}T|_{T_{av}+f}+\text{grad}T|_{T_{av}-f})-\text{grad}T|_{T_{\text{av}}}] \tag{4}$$

where k_{warm} is the equivalent thermal conductivity of the soil layer ranging from the ground surface to the depth of d. Considering that $d\gg\varepsilon$, Eq. 4 becomes

$$\Delta q_{\text{warm}}=k_{warm}\times\frac{f\varepsilon}{d^2}. \tag{5}$$

Equation 5 suggests that in warm season, considering the effect of DTFA results in more warm energy being penetrated to the underlying soil than ignoring that effect.

Heat flow difference between ignored and considered DTFA in cold season

In cold season, the heat flow difference between the ignored and the considered DTFA is Δq_{cold}. To calculate Δq_{cold}, three steps need to be done. First, refer the time of $T=T_{\text{av}}$ in warm season to the time of $T=-T_{av}+2\times T_0$ in cold season using Eq. 1. It is noted that this reference is a one-by-one function because of the anti-symmetric characteristics of seasonal sinusoid function. For instance, in Fig. 8, point B is referred to point A. Second, evaluate whether in Eq. 2 the parameter d in point B is equal to that in point A. Set d in warm season as d_{w} and in cold season as d_{c}. If the average annual temperature T_0 shown in Eq. 1 is exactly 0°C, then $d_{\text{w}}=d_{\text{c}}$. In permafrost region $T_0<0$; thereby, d_{c} is theoretically greater than d_{w}. In the Qinghai–Tibet plateau $-3.5<T_0<0$ (Wang and French 1994), it thus has $d_{\text{w}}\approx d_{\text{c}}=d$. Third, do the same process from Eqs. 2, 3, 4, and 5 and note that the sign of ε in Eq. 3 has to be changed from positive to negative and from negative to positive. Having done these three steps, we have:

$$\Delta q_{cold}=-k_{cold}\times\frac{f\varepsilon}{d^2}. \tag{6}$$

Equation 6 signifies that considering the effect of DTFA results in more cold energy being transferred downward to the underlying soil than ignoring that effect.

Thermal budget after considering the effect of DTFA

The net cold energy is positive when the DTFA effect on geo-temperature is counted. The thermal conductivity of unfrozen soil is greater than of frozen soil because ice conductivity is approximately four times that of water conductivity. In cold season, the free moisture in the soil near the ground surface is partially frozen; the thermal conductivity of this soil increases. Thus, it is true that $k_{\text{cold}}>k_{\text{warm}}$ (Cheng et al. 2008a; French 2007). Therefore, the different heat flow between the ignored and the considered DTFA, Δq, during the two anti-symmetric times (the special time in warm season B and its referred time in cold season A) is:

$$\Delta q=-(k_{cold}-k_{warm})\frac{f\varepsilon}{d^2}<0. \tag{7}$$

Summating Eq. 7 in all the time of a given year yields the annual thermal budget difference between the ignored and the considered DTFA. This summation is of negative magnitude, indicating that not considering the low DTFA on geo-temperature overestimates the warming of the underlying soil; that is, the existence of low DTFA can maintain the underlying soil in a cool stage.

High DTFA

When the DTFA is of high magnitude, a residual warm energy is stored in the underlying soil because the penetrated warm energy partially thaws the shallow permafrost layer. In warm season, a high DTFA results in a high positive thermal gradient near the ground surface, facilitating the warm energy to partially thaw the underlying permafrost and thus making the warm energy stored. In cold season, the high negative thermal gradient near the ground surface allows the cold energy to penetrate to and through the permafrost layer because the permafrost's thermal conductivity in cold season is greater than that in warm season. The store of cold energy is thus less than of warm energy. In the high DTFA region, this unequal energy store results in the underlying permafrost being warmed.

Discussion

Specific DTFA for different ground surfaces

The current model which does not take the DTFA into consideration has overestimated the warming of the underlying soil. In fact, the DTFA of the boundary condition T_1 in Fig. 2 is quite lower compared to the boundary condition T_2 because the natural ground (T_1) is covered by vegetation while the embankment surface and slope (T_2) are bald.

When the geothermal regime under asphalt or PCC pavement is estimated, not considering the effect of DTFA will underestimate the warming of the underlying permafrost. The dark color of asphalt pavement and gray color PCC slab absorb considerable solar heat at noon; the DTFA of these pavement surfaces is therefore usually >12°C (Yu et al. 1998).

Maintaining the DTFA on the embankment surface and slope at approximately 5°C is an alternative to ensure the stability of the permafrost under roadway embankment. If the DTFA on the embankment surface is 5°C (Figs. 3, 4, and 5), the soil under the embankment can maintain in a cooler stage in the long run compared with the embankment surface with 0°C, 8°C, or 12°C DTFAs.

Limitation of this study

To investigate the effects of DTFA on the geo-temperature of the underlying soil in the permafrost region, the daily temperature is assumed to approximate a sinusoidal wave. This approximation makes sense if the daily weather does not significantly vary (Armagahni et al. 1987). However, when the daily weather significantly changes, for instance, from sunny to rainy, using sinusoidal function to approximate the real temperature leads to considerable error.

Conclusion

1. The DTFA cannot change the seasonal geo-temperature fluctuation, but can significantly change the magnitude of the geo-temperature. When the DTFA is ignored in the computational model, the warming of the underlying soil is overestimated if the DTFA is of comparatively low magnitude such as 5°C or 8°C, but underestimated if the DTFA is of a high magnitude such as 12°C.
2. The soil's thermal conductivity in cold season is larger than that in warm season, resulting in the absorbed cold energy in cold season being larger than the absorbed warm energy in warm season. Therefore, lower DTFA can maintain the underlying permafrost in a cool state.
3. High DTFA results in that, in warm season, warm energy partially thaws the underlying permafrost layer. This phase change leads to warm energy being stored in the permafrost layer. High DTFA is therefore deleterious to the stability of the permafrost under the roadway embankment.

References

Andersland OB, Ladanyi B (1994) An introduction to frozen ground engineering. Chapman & Hall, New York

Armagahni JM, Larsen TJ, Smith LL (1987) Temperature response of concrete pavements. J Trans Res Board 1121:23–33

Cheng G, Sun Z, Niu F (2008) Application of the roadbed cooling approach in Qinghai–Tibet railway engineering. Cold Reg Sci Technol 53(3):241–258

Chenji H, Doushun, Qianzeyu (2006) Yin-Yang Slope problem along Qinghai–Tibetan Lines and its radiation mechanism. Cold Reg Sci Technol 44(3):217–224

French HM (2007) The periglacial environment. Wiley, West Sussex

Li G, Li N, Quan X (2006) The temperature features for different ventilated-duct embankments with adjustable shutters in the Qinghai–Tibet railway. Cold Reg Sci Technol 44(2):99–110

Li G, Li N, Kang J (2007) Heat transfer characteristics of the embankment with crushed-rock slope protection in permafrost regions along the Qinghai–Tibet Railway. Journal of Glaciology and Geocryology 29(2):315–321 (in Chinese)

Li S, Lai Y, Zhang M, Dong Y (2009) Study on long-term stability of Qinghai–Tibet Railway embankment. Cold Reg Sci Technol 57 (2–3):139–147

Ma W, Qi J, Wu Q (2008) Analysis of the deformation of embankments on the Qinghai–Tibet Railway. J Geotech Geoenviron Eng 134 (11):1645–1654

Qin D (2002) Assessment on the environment in Western China. Science Press, Beijing

Qin Y, Zheng B (2010) The Qinghai–Tibet Railway: a landmark project and its subsequent environmental challenges. Environ, Dev Sustain. doi:10.1007/s10668-009-9228-x

Qin Y, Zhang J, Li G, Qu G (2010) Settlement characteristics of unprotected embankment along the Qinghai–Tibet Railway. Cold Reg Sci Technol 60(1):84–91

Quan X, Li N, Li G (2006) A new ripraped-rock slope for high temperature permafrost regions. Cold Reg Sci Technol 45 (1):42–50

Wang B, French HM (1994) Climate controls and high-altitude permafrost, Qinghai–Xizang (Tibet) Plateau, China. Permafrost Periglac Process 5(2):87–100

Ya-ling C, Yu S, Zhen-ming W, Wei M (2008) Calculation of temperature differences between the sunny slopes and the shady slopes along railways in permafrost regions on Qinghai–Tibet Plateau. Cold Reg Sci Technol 53(3):346–354

Ya-ling C, Yu S, Zhen-ming W (2009) Evaluation on thermal stability of embankments with different strikes in permafrost regions. Cold Reg Sci Technol 58(3):151–157

Yu HT, Khazanovich L, Darter MI, Ardani A (1998) Analysis of concrete pavement responses to temperature and wheel loads measured from instrumented slabs. Transportation Research Record: J Trans Res Board 1639:94–101

Yu Q, Pan X, Cheng G, He N (2008) An experimental study on the cooling mechanism of a shading board in permafrost engineering. Cold Reg Sci Technol 53(3):298–304

Zhang J (2007) Estimation on the settlement and deformation of embankment along Qinghai–Tibet Railway in permafrost regions. Hongguo Tiedao Kexue/China Railway. Science 28(3):12–17

Zhang M, Lai Y, Liu Z, Gao Z (2005a) Nonlinear analysis for the cooling effect of Qinghai–Tibetan Railway embankment with different structures in permafrost regions. Cold Reg Sci Technol 42(3):237–249

Zhang M, Zhang J, Lai Y (2005b) Numerical analysis for critical height of railway embankment in permafrost regions of Qinghai–Tibetan Plateau. Cold Reg Sci Technol 41(2):111–120

Zhang T, Baker THW, Cheng G-D, Wu Q (2008) The Qinghai–Tibet Railroad: a milestone project and its environmental impact. Cold Reg Sci Technol 53(3):229–240

Zheng B, Zhang J, Qin Y (2010) Investigation for the deformation of embankment underlain by warm and ice-rich permafrost. Cold Reg Sci Technol 60(2):161–168